Biochemistry and Biophysics Reports 40 (2024) 101818

Contents lists available at ScienceDirect

Biochemistry and Biophysics Reports

journal homepage: www.elsevier.com/locate/bbrep

Asparagus racemosus silver chloride nanoparticles and *Kaempferia rotunda* mediated silver/silver chloride nanoparticles inhibit human hepatocellular and lung cancer cell lines

Syed Rashel Kabir [a,*], Mohammad Taufiq Alam [b], Md Belal Uddin [a]

[a] Department of Biochemistry and Molecular Biology, Faculty of Science, University of Rajshahi, Rajshahi, 6205, Bangladesh
[b] Department of Applied Chemistry and Chemical Engineering, University of Rajshahi, Rajshahi, 6205, Bangladesh

ARTICLE INFO

Keywords:
Biogenic silver nanoparticles
Lung cancer cell
Apoptosis
Cell cycle
Cell
Liver cancer cell

ABSTRACT

Recently, we have reported that biogenic silver/silver chloride nanoparticles from *Asparagus racemosus* (*A. racemosus*-AgCl-NPs) and *Kaempferia rotunda* (*K. rotunda*-Ag/AgCl-NPs) inhibited different cancer cells by inducing apoptosis and several genes alteration. Here for the first time, we assessed the effects of these two nanoparticles on human lung (A549) and hepatocellular (SMMC-7721) carcinoma cell lines. *A. racemosus*-AgCl-NPs and *K. rotunda*-Ag/AgCl-NPs inhibited A549 cell growth with IC_{50} values of 22.7 and 59.7 μg/ml and the calculated IC_{50} values for SMMC-7721 cell were 89.3 and 126.3 μg/ml, respectively. *A. racemosus*-AgCl-NPs exerted higher cytotoxicity against HEK293T cells than doxorubicin and *K. rotunda*-Ag/AgCl-NPs. Both the nanoparticles induced apoptosis in A549 and SMMC-7721 cell lines. A significant rise of early apoptotic cells and late apoptotic cells was found for A549 cells after treatment with *A. racemosus*-AgCl-NPs and stained with FITC-annexin V/PI. Apoptosis in A549 cells was further confirmed by monitoring the alteration of the expression level of several genes using real-time PCR and cell cycle arrest by flowcytometry after treatment with *A. racemosus*-AgCl-NPs. The expression of STAT-3, TNFα, and EGFR genes was decreased with the increase of caspase-8, FAS, and FADD gene expression. G_2/M cell cycle phase was arrested after treatment of A549 cells with *A. racemosus*-AgCl-NPs.

1. Introduction

Cancer remains a leading cause of mortality, with over 100 types currently identified. In 2022, the United States alone reported 1.9 million new cancer cases, resulting in 609,360 deaths. Lung and bronchial cancer are particularly deadly, with lung cancer ranking as the second most common cancer worldwide, following breast cancer. Conventional chemotherapeutic drugs often have severe side effects and can lead to drug resistance, prompting researchers to seek alternative treatments. Biogenic nanoparticles have recently garnered attention for their potential anticancer properties. In our research, we synthesized and characterized biogenic silver/silver chloride nanoparticles using *Asparagus racemosus* (*A. racemosus*-AgCl-NPs) and *Kaempferia rotunda* (*K. rotunda*-Ag/AgCl-NPs), which demonstrated anticancer activity against several cancer cell lines [1–6]. Specifically, these nanoparticles inhibited the proliferation of human glioblastoma stem cancer cells (GSC-3) *in vitro* and Ehrlich ascites carcinoma (EAC) cells *in vivo* [3,6], as well as human pancreatic (BxPC-3) and breast cancer (MCF-7) cells [4].

Although the anticancer effects of some biogenic silver nanoparticles against the A549 human lung cancer cell line have been reported [7–14], the underlying molecular mechanisms remain largely unexplored. In continuation of our previous work, we now report for the first time that *A. racemosus*-AgCl-NPs and *K. rotunda*-Ag/AgCl-NPs inhibit the growth of hepatocellular carcinoma (SMMC-7721) and lung cancer (A549) cell lines. Furthermore, we elucidate the molecular mechanisms behind the anticancer properties of *A. racemosus*-AgCl-NPs.

2. Materials and methods

2.1. Synthesis of silver nanoparticles

A. racemosus-AgCl-NPs and *K. rotunda*-Ag/AgCl-NPs were synthesized according to the established protocol [3,6] and stored at 4 °C.

* Corresponding author.
E-mail addresses: rashelkabir@ru.ac.bd, rashelkabir@gmail.com (S.R. Kabir).

https://doi.org/10.1016/j.bbrep.2024.101818
Received 6 December 2023; Received in revised form 4 August 2024; Accepted 28 August 2024

2.2. Cytotoxicity study against SMMC-7721, A549 and HEK293T cells

Human lung A549, hepatocellular carcinoma SMMC-7721, and Human embryonic kidney HEK293T cells were recruited from the American Type Culture Collection (ATCC). At first DMEM medium was prepared using DMEM powder with high glucose (Gibco), FBS (Gibco), $NaHCO_3$, HEPES (Carl Roth, Germany), and antibiotics (Amresco). The stored cells were kept at 37 °C for a short period and then cells were added to 9.0 ml of DMEM medium, centrifuged (Eppendorf) and collected cells were added to 5 ml of DMEM medium with high glucose and subcultured in T-25 cell culture flax containing DMEM medium using CO_2 incubator at 37 °C (Galaxy 170 S, New Brunswick). When cells reached around 90 % confluency, trypsin-EDTA (Gibco) was added to the flax and incubated. Finally, detached cells were counted by an inverted microscope (Euromex). A549 (10,000/well), HEK293T (10,000/well) and SMMC-7721 (20,000/well) cells were seeded in 96-well cell culture plates. After 24 h, A549 cells were treated with 16.0–64.0 μg/ml concentration of *A. racemosus*-AgCl-NPs and *K. rotunda*-Ag/AgCl-NPs whereas SMMC-7721 cells were treated with both the nanoparticles at the concentration range from 32.0 to 128 μg/ml for 48 h. HEK293T cells were treated with *A. racemosus*-AgCl-NPs, *K. rotunda*-Ag/AgCl-NPs, and cancer drug doxorubicin at the concentration of 2–16 μg/ml for 48h. Then MTT, (3-[4,5-dimethylthiazole-2-yl]-2,5-diphenyltetrazolium bromide) bought from Carl Roth, Germany, was added and kept in a CO_2 incubator at 37 °C. About 3 h later, crystals were dissolved using isopropanol containing 0.1 N HCl and absorbances were recorded at 630 nm using BioTek 800 TS microplate reader. Finally, MS Excel software was used to calculate growth inhibition and IC_{50} values.

2.3. Detection of apoptosis by Hoechst 33342 stain

A549 cells (40,000/well) were seeded in a 24 wells cell culture plate and were treated with *A. racemosus*-AgCl-NPs and *K. rotunda*-Ag/AgCl-NPs at the concentration of 32 μg/ml while SMMC-7721 cells (80,000/well) were treated with the nanoparticles at the concentrations of 64 μg/ml 24 h later medium was taken out and the attached cells were washed with PBS (phosphate buffer saline). After that cells were stained with Hoechst 33342. Finally, to detect apoptosis cell morphological alterations were observed, and the pictures were captured using a fluorescence microscope (Olympus IX71).

2.4. Detection of death cells by flowcytometry

A549 cells (5×10^5) were seeded in the T-25 flask and 24 h later treated with *A. racemosus*-AgCl-NPs (64 μg/ml). After that cells were detached and washed with the annexin V binding buffer. Then cells were incubated with FITC-annexin V/PI (Invitrogen) for about 20 min in the dark at room temperature. Finally, apoptotic cell death was detected by using a CytoFLEX flow cytometer (Beckman coulter).

2.5. Cell cycle analysis

A549 cells were cultured and treated with *A. racemosus*-AgCl-NPs (64 μg/ml) for 48 h as represented above. After detaching, cells were stored using PBS and 70 % alcohol for 24 h. Then cells were washed three times with PBS and incubated in 1 ml PBS for 30 min with 50 μl of RNase A (1.0 mg/ml) at 37 °C. Finally, cell cycle phases were detected by a CytoFLEX flow cytometer after the addition of 5 μl of propidium iodide (1.0 mg/ml).

2.6. Gene expression

A549 cells were treated with *A. racemosus*-AgCl-NPs (64 μg/ml) for 24 h as described above and RNA was isolated according to the manufacturer's instruction (FAVORGEN, Taiwan). Then cDNA was constructed and mixed with 2 × SYBR green master mix according to the manufacturer (TsingKe, China) supplied protocol. Expression levels of STAT-3, TNFα, EGFR, Caspase-8, FAS, and FADD were detected by a BIO-RAD Real-Time thermal cycler (CFX96). The PCR condition was set to 50 °C for 2 min 95 °C for 3 min followed by 40 cycles at 95 °C for 15 s and 60 °C for 1 min. Primers were designed according to Kabir et al. [2–4], and bought from TsingKe, China (Table 1).

3. Result

3.1. Cytotoxicity test by MTT assay

At the concentration of 16 μg/ml of *A. racemosus*-AgCl-NPs 43 % of A549 cell growth was inhibited. When the concentration was increased to 32 and 64 μg/ml, cell growth inhibition was increased to 60 % and 73 %, respectively (Fig. 1A). Similarly, *K. rotunda*-Ag/AgCl-NPs inhibited 9.3 %, 39.1 %, and 49.8 % of A549 cell growth at the concentrations of 16, 32 and 64 μg/ml, respectively (Fig. 1A). The IC_{50} value was calculated for A549 cell to be 22.7 μg/ml for *A. racemosus*-AgCl-NPs and 59.7 μg/ml for *K. rotunda*-Ag/AgCl-NPs. On the other hand, *A. racemosus*-AgCl-NPs inhibited 22.7 %, 34.5 %, and 70.5 % of SMMC-7721 cell growth at the concentration of 32, 64, and 128 μg/ml respectively (Fig. 1B). While *K. rotunda*-Ag/AgCl-NPs inhibited only 8.2 % and 53 % SMMC-7721 cells growth at the concentration of 64 and 128 μg/ml (Fig. 1B). The IC_{50} value was calculated for SMMC-7721 cell to be 89.3 μg/ml for *A. racemosus*-AgCl-NPs and 126.3 μg/ml for *K. rotunda*-Ag/AgCl-NPs respectively. Like SMMC-7721 and A549 cells, HEK293T cell growth inhibition was also dose-dependent. In the presence of 16 μg/ml of *A. racemosus*-AgCl-NPs, doxorubicin and *K. rotunda*-Ag/AgCl-NPs 60.2 %, 50.6 %, and 49.5 % HEK293T cells growth were inhibited respectively. The value decreased gradually with the decrease of concentration (Fig. 1C). The IC_{50} value was calculated for HEK293T cell to be 9.3, 15.8, and 16.0 μg/ml for *A. racemosus*-AgCl-NPs, *K. rotunda*-Ag/AgCl-NPs, and doxorubicin, respectively.

3.2. Study of morphological changes by Hoechst 33342 dye

After treatment with *A. racemosus*-AgCl-NPs and *K. rotunda*-Ag/AgCl-NPs, both cells were stained with Hoechst 33342 and the fluorescence microscopic images indicated condensed nuclear in A549 and SMMC-7721 cells as compared with untreated A549 and SMMC-7721 cells (Fig. 2). Apoptosis is a program cell death. The common features of apoptosis are DNA degeneration, cell shrinkage, membrane blebbing, chromosome condensation, and nuclear fragmentation. Our results indicate that the nanoparticles induced apoptosis both in A549 and SMMC-7721 cells.

3.3. Detection of death cells by flowcytometry

Early and late apoptotic cells were detected by using a flow

Table-1
Primer List.

18s [4]	F	GTAACCCGTTGAACCCCATT
	R	CCATCCAATCGGTAGTAGCG
STAT-3 [3]	F	CAGCAGCTTGACACACGGTA
	R	AAACACCAAAGTGGCATGTGA
TNFα [4]	F	ATTGCCGCAGAAAGTTCTACG
	R	GTCCAGTTTCGTCTTCAGCTC
FAS [4]	F	CCCAGTCCTTCACTTCTATGTTC
	R	GTAGCACAGTTCAGTCTCGAC
Caspase-8 [4]	F	ACACAGTCGAGTAGACTCTCAAA
	R	AGGAAGTGATGCTCGTTCAGA
EGFR [3]	F	AGGCACGAGTAACAAGCTCAC
	R	ATGAGGACATAACCAGCCACC
FADD [2]	F	GCTGGCTCGTCAGCTCAAA
	R	ACTGTTGCGTTCTCCTTCTCT

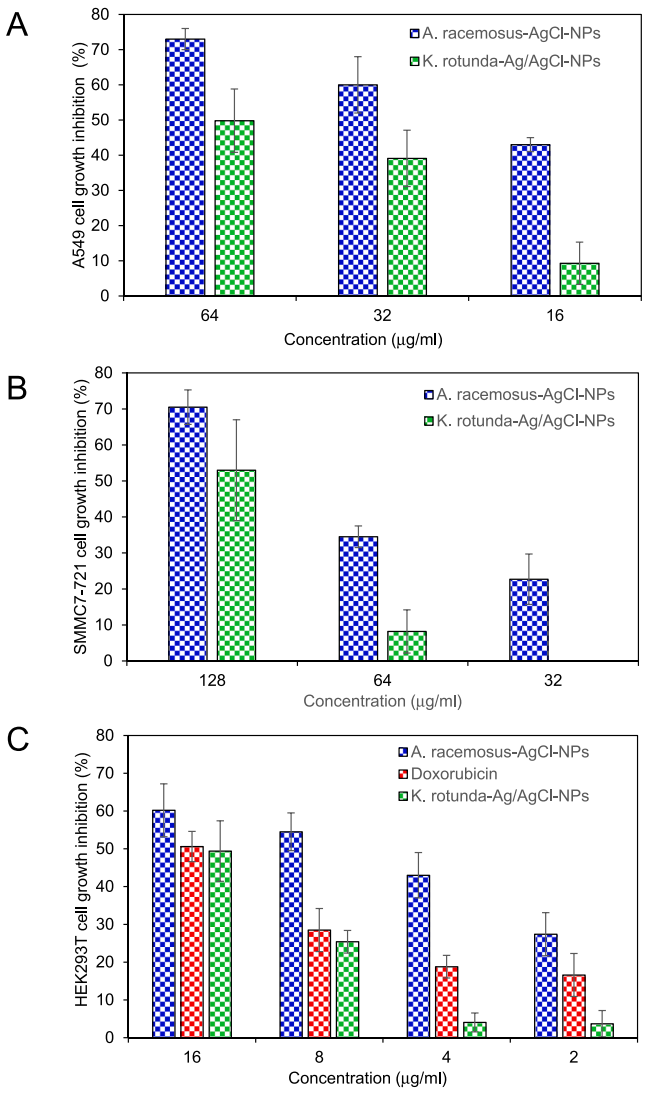

Fig. 1. Antiproliferative activity of *A. racemosus*-AgCl-NPs and *K. rotunda*-Ag/AgCl-NPs against A549, SMMC-7721 and HEK293T cells. (A) represents the effect of *A. racemosus*-AgCl-NPs and *K. rotunda*-Ag/AgCl-NPs against A549 cells; (B) indicate the effects of *A. racemosus*-AgCl-NPs and *K. rotunda*-Ag/AgCl-NPs against SMMC-7721 cells; (C) represents the effects of *A. racemosus*-AgCl-NPs, *K. rotunda*-Ag/AgCl-NPs and doxorubicin against HEK293T cells. (n = 3 and mean ± S.D).

cytometer. Before treatment, 92.71 % live A549 cells, 0.25 % early apoptotic cells, 1.09 % late apoptotic cells, and 5.95 % necrotic cells were observed. After treatment with *A. racemosus*-AgCl-NPs the number of early apoptotic cells, and late apoptotic cells was increased to 0.91 % and 4.59 %, respectively with a significant increase of necrotic death cells to 34.38 % (Fig. 3).

3.4. Alteration of gene expression in A549 cells

Apoptosis is the process of programmed cell death that is caused by the change of expression level of multiple genes. In this study, we checked the expression level of STAT-3, TNFα, EGFR, Caspase-8, FAS, and FADD gene in A549 cells after treatment with *A. racemosus*-AgCl-NPs. We observed STAT-3, TNFα, and EGFR gene expression was decreased with the increase of Caspase-8, FAS, and FADD gene expression. (Fig. 4).

3.5. Detection of changes in cell cycle phases in A549 cells

After treatment of A549 cells with *A. racemosus*-AgCl-NPs, the sub-G_1 phase increased significantly. In this late stage of the apoptosis process, DNA degrades into small fragments. The G_0/G_1 cell cycle phase reduced with the notable increase of S and G_2/M phases compared with the untreated A549 cells (Fig. 5 A&B).

4. Discussion

Cytotoxicity of several biogenic silver nanoparticles against lung cancer cell line A549 was investigated and reported at different degrees [7–12,15]. Although cytotoxicity of biogenic silver nanoparticles against A549 cells was reported in about a dozen papers, only one paper reported the anticancer effects against SMMC-7721 cells [16]. *A. racemosus*-AgCl-NPs and *K. rotunda*-Ag/AgCl-NPs inhibited the proliferation of A459 and SMMC-7721 cancer cells. *A. racemosus*-AgCl-NPs showed stronger cytotoxicity in both types of cancer cell lines than *K. rotunda*-Ag/AgCl-NPs and among the two cells, A549 was more sensitive towards *A. racemosus*-AgCl-NPs. Besides the cancer cell lines, the cytotoxicity of the nanoparticles was also checked against the human embryonic kidney cell line (HEK293T). The data revealed that *A. racemosus*-AgCl-NPs was more toxic than cancer drug doxorubicin and *K. rotunda*-Ag/AgCl-NPs.

Some mechanisms caused the decrease of cell growth after treatment with various agents. Apoptosis or programmed cell death is one of them. During apoptosis, various changes are observed in the cells. One of these changes is DNA fragmentation or condensation. Condensed nuclei were detected both in the A549 and SMMC-7721 cells after treatment with *A. racemosus*-AgCl-NPs and *K. rotunda*-Ag/AgCl-NPs by staining with Hoechst 33342. Although cytotoxicity was reported for several biogenic silver nanoparticles against A549 cells, apoptotic-induced cell death was reported only for, *Garcinia atroviridis* leaf extract [7] and *Artemisia oliveriana* extract [13] silver nanoparticles. On the other hand, *Taxus yunnanensis* callus extract mediated AgNPs induced apoptosis in SMMC-7721 cells [16]. Apoptosis can be late or early stages. In this study, early and late apoptosis was detected in A549 cells by FITC-annexin V/PI staining and using flow cytometry after treatment with the *A. racemosus*-AgCl-NPs. The number of early and late apoptotic cells increased significantly.

Apoptosis is associated with the alteration of various genes involved in several pathways. Based on our previous experiments [2–4,6], we have targeted some pathways in this study. Here STAT-3, TNFα, EGFR gene expression was downregulated with the upregulation of Caspase-8, FAS, and FADD gene expression. STAT-3 can inactivate both the intrinsic and extrinsic apoptotic pathways and thereby resist radiation and cytotoxic drugs, against cancer cells [17]. Moreover, activation of STAT-3 is correlated with various cellular processes in non-small cell lung cancer [18]. Lung cancer contains a few cancer stem cells that retain the capability of repopulation [19]. STAT-3 helps to retain the self-renewal capacity of cancer stem cells. So, downregulation of STAT-3 can be a way of controlling cancer cell growth. In the present experiment, expression of STAT-3 was decreased after treatment with the *A. racemosus*-AgCl-NPs. In our previous experiments [3,6] it was found that *K. rotunda*-Ag/AgCl-NPs and *A. racemosus*-AgCl-NPs down-regulate the STAT3 gene and some other genes and cause the apoptosis in human glioblastoma stem cells.

Activated EGFR plays cardinal roles in cell proliferation, differentiation, migration, and apoptosis by exciting the subsequent intracellular signaling pathways [20]. EGFR can activate STAT-3 [19]. In the present study, the expression of EGFR was decreased as a result, the expression of STAT-3 was also decreased. A similar result was also observed for GSC-3 after treatment with *K. rotunda*-Ag/AgCl-NPs and *A. racemosus*-AgCl-NPs [3,6].

Tumor necrosis factor (TNFα) is a pro-inflammatory cytokine that plays critical functions in diverse cellular events for example cell

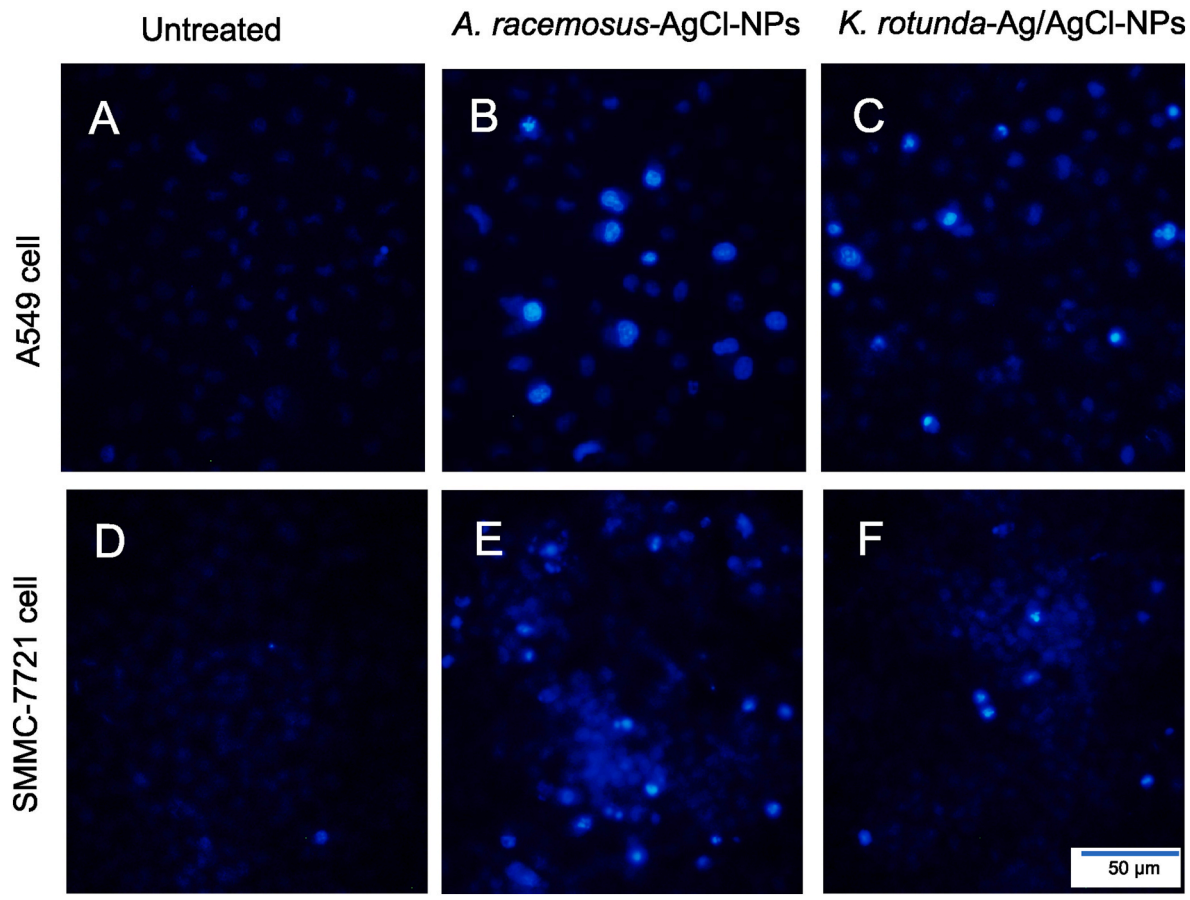

Fig. 2. Morphological study of *A. racemosus*-AgCl-NPs and *K. rotunda*-Ag/AgCl-NPs treated A549 and SMMC-7721 cells staining with Hoechst 33342 dye. (A) and (D) represent untreated A549 and SMMC-7721 cells, respectively. (B) and (E) show *A. racemosus*-AgCl-NPs treated A549 and SMMC-7721 cells, respectively. (C) and (F) indicating *K. rotunda*-Ag/AgCl-NPs treated A549 and SMMC-7721 cells, respectively.

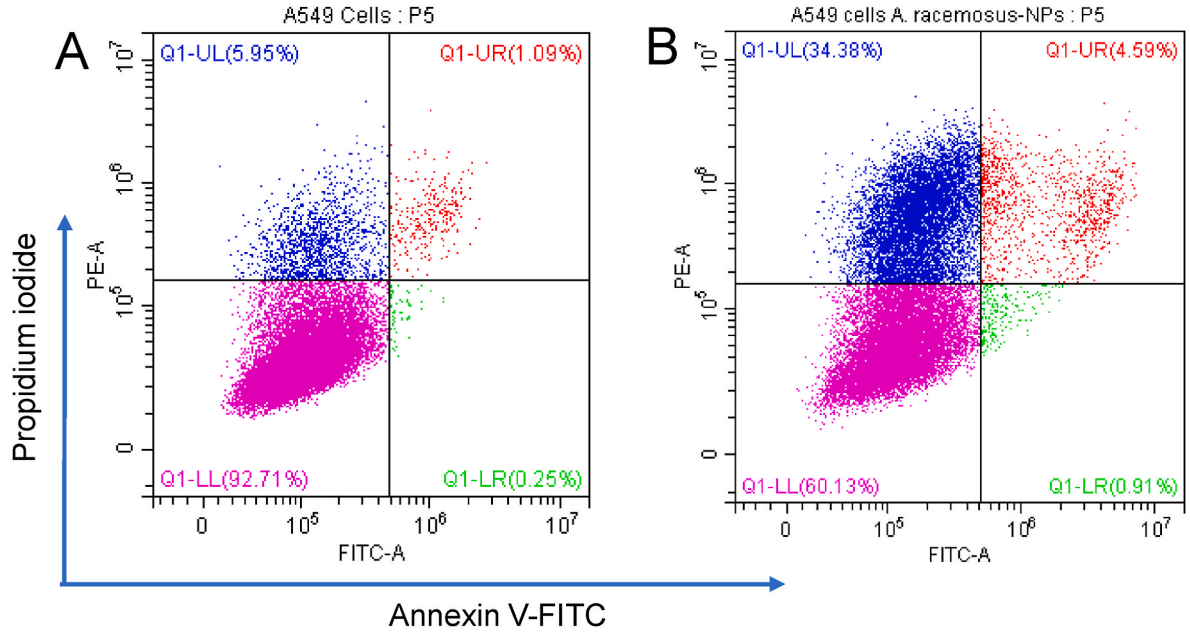

Fig. 3. Detection of early and late apoptosis by staining with annexin-V/PI after treatment of A549 cells with *A. racemosus*-AgCl-NPs. (A) represents untreated A549 cells whereas (B) represents *A. racemosus*-AgCl-NPs treated A549 cells. Q1-LL, Q1-LR, Q1-UR, and Q1-UL indicate live cells, early apoptotic cells, late apoptotic cells, and necrotic cells, respectively.

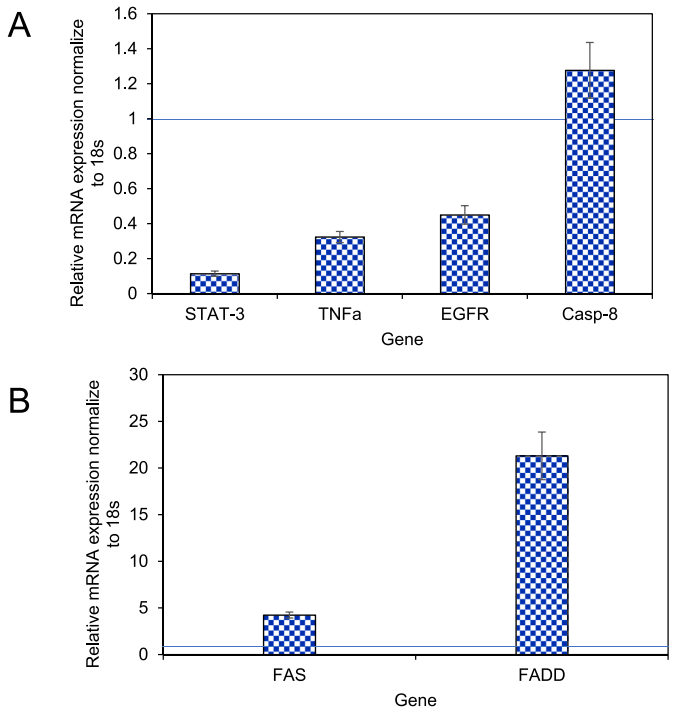

Fig. 4. Alteration of gene expression after treatment of A549 with *A. racemosus*-AgCl-NPs detected by real-time PCR. (A) Relative mRNA expression of STAT-3, TNFα (TNFa), EGFR, and Caspase-8 (Casp-8). Similarly, (B) represents the expression level of FAS and FADD genes. The blue line indicates the 1.0 expression level. (For interpretation of the references to colour in this figure legend, the reader is referred to the Web version of this article.)

proliferation, survival, differentiation, and death. Here expression of the TNFα gene was downregulated in A549 cells after treatment with 64 μg/ml concentration of *A. racemosus*-AgCl-NPs. The opposite result was observed for GSC-3 cells [6], where 8 μg/ml concentration of *A. racemosus*-AgCl-NPs increased the expression of the TNFα gene that activated NFκB through the activation of the IKK gene and caused apoptotic cell death of GSC-3. Silver nanoparticles have a dual effect showing both inflammatory and anti-inflammatory effects [21,22]. This effect may be correlated with the concentration of silver nanoparticles. It was reported that at 1 μM concentration of green silver nanoparticles, expression of TNFα increased significantly [23]. In a different experiment, it was reported that expression of TNFα decreased with the increase of silver nanoparticle concentration, and at 100 μM concentration expression reached a minimum level [24]. Increased concentration of silver nanoparticles decreased the expression of TNFα receptor-1 which may reduce TNFα-induced signal transduction in a lung epithelial cell line [21].

Several internal and external incidences of cells stimulate the apoptosis process. The extrinsic pathway is one of those that is mediated by the death receptor e.g. FAS. During apoptosis, FAS formed a complex with FADD and Procaspase-8 known as DISC (Death-inducing signaling complex) and the Procaspase-8 through the self-cleavage to active Caspase-8. Then the activated Caspase-8 activated Procaspase-3 by cleaving it directly. The activated Caspase-3 then breaks down DNA by activating other proteins and causing apoptosis in cells [25]. Here FAS, FADD, and Caspase-8 expression increased in A549 cells after treatment with *A. racemosus*-AgCl-NPs state the possibility of the involvement of extrinsic apoptosis pathways. The gene expression results were pictorially represented in Fig. 6. *Artemisia oliveriana* extract-mediated silver nanoparticles altered the BAX, BCL-2, and Caspase-3 gene expression in A549 cells [13] stating the possibility of involvement of intrinsic mitochondrial pathway. Induction of apoptosis by the activation of extrinsic pathways was observed when *Z. mauritiana* fruits mediated Ag/AgCl-NPs treated with MCF-7 cells [2].

The cell cycle in each cell is very important for its survival. Apoptosis can be induced by arresting any of the cell cycle phases. Here G_0/G_1 phase decreased significantly with the remarkable increase of S and G_2/M phases in A549 cells after treatment with *A. racemosus*-AgCl-NPs. Besides the cell cycle arrest in G_2/M phase, the population in the sub-G_1 phase increased significantly which represents apoptotic cells. In this experiment, FADD expression increased remarkably which may be co-related with G_2/M phase arrest [26].

In conclusion, both the *A. racemosus*-AgCl-NPs and *K. rotunda*-Ag/AgCl-NPs inhibited the growth of A549 and SMMC-7721 cells by inducing apoptosis. In both cell lines *A. racemosus*-AgCl-NPs was more cytotoxic than *K. rotunda*-Ag/AgCl-NPs, and A549 was more sensitive towards *A. racemosus*-AgCl-NPs than that of the SMMC-7721 cells. *A. racemosus*-AgCl-NPs induced apoptosis by reducing the expression of some key genes responsible for cell proliferation, differentiation, migration, and other cellular processes and by activating the extrinsic apoptotic pathways and G_2/M cell cycle arrest.

Data availability statement

Not applicable.

Competing interests/COI statement

The author declares no competing interests.

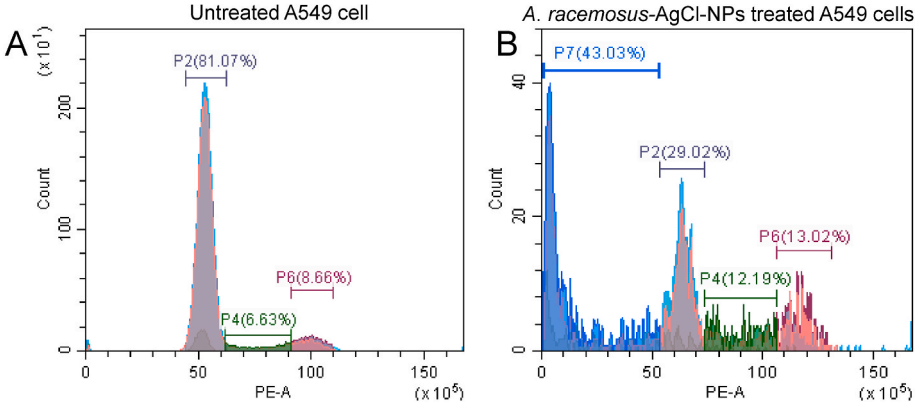

Fig. 5. Detection of A549 cell cycle arrest after treatment with *A. racemosus*-AgCl-NPs. (A) P2, P4 and P6 indicating G_0/G_1, S and G_2/M phases of untreated A549 cells, respectively. (B) p7, P2, P4 and P6 indicate sub G_1, G_0/G_1, S and G_2/M phases, respectively.

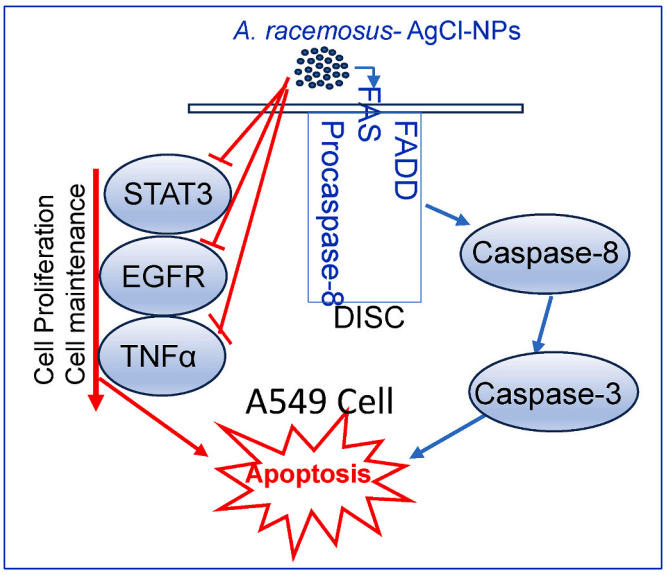

Fig. 6. Cartoon representation of the gene expression results.

Ethics approval statement

Not applicable.

Funding

This research work is funded by the Faculty of Science, University of Rajshahi (Grant No. 529/5/52/RU/Science-20/18-19/72).

CRediT authorship contribution statement

Syed Rashel Kabir: Writing – review & editing, Writing – original draft, Resources, Investigation, Funding acquisition, Conceptualization. **Mohammad Taufiq Alam:** Resources, Writing – review & editing, Investigation. **Md Belal Uddin:** Funding acquisition.

Declaration of competing interest

The authors declare that they have no known competing financial interests or personal relationships that could have appeared to influence the work reported in this paper.

N/A.

References

[1] A.K.M. Asaduzzaman, B. Chun, S.R. Kabir, Vitis vinifera assisted silver nanoparticles with antibacterial and antiproliferative activity against Ehrlich ascites carcinoma cells, J. Nanoparticles. 2016 (2016).

[2] S.R. Kabir, A. Asaduzzaman, R. Amin, A.T. Haque, R. Ghose, M.M. Rahman, J. Islam, M.B. Amin, I. Hasan, T. Debnath, B.-S. Chun, X. Zhao, M.K.R. Khan, M. T. Alam, Zizyphus mauritiana fruit extract-mediated synthesized silver/silver chloride nanoparticles retain antimicrobial activity and induce apoptosis in MCF - 7 cells through the fas pathway, ACS Omega 5 (2020) 20599–20608, https://doi.org/10.1021/acsomega.0c02878.

[3] S.R. Kabir, Z. Dai, M. Nurujjaman, X. Cui, A.K.M. Asaduzzaman, B. Sun, X. Zhang, H. Dai, X. Zhao, Biogenic silver/silver chloride nanoparticles inhibit human glioblastoma stem cells growth in vitro and Ehrlich ascites carcinoma cell growth in vivo, J. Cell Mol. Med. 24 (2020) 13223–13234, https://doi.org/10.1111/jcmm.15934.

[4] S.R. Kabir, F. Islam, A.K.M. Asaduzzaman, Biogenic silver/silver chloride nanoparticles inhibit human cancer cells proliferation in vitro and Ehrlich ascites carcinoma cells growth in vivo, Sci. Rep. 12 (2022) 1–14, https://doi.org/10.1038/s41598-022-12974-z.

[5] R. Ghose, A.K.M. Asaduzzaman, I. Hasan, S.R. Kabir, Hypnea musciformis-mediated Ag/AgCl-NPs inhibit pathogenic bacteria, HCT-116 and MCF-7 cells' growth in vitro and Ehrlich ascites carcinoma cells in vivo in mice, IET Nanobiotechnol. 16 (2022) 49–60, https://doi.org/10.1049/nbt2.12075.

[6] S.R. Kabir, F. Islam, A.A. Al-bari, A.K.M. Asaduzzaman, Asparagus racemosus mediated silver chloride nanoparticles induce apoptosis in glioblastoma stem cells in vitro and inhibit Ehrlich ascites carcinoma cells growth in vivo, Arab. J. Chem. 15 (2022) 104013, https://doi.org/10.1016/j.arabjc.2022.104013.

[7] M. Muhamad, N.A. Rahim, W.A.W. Omar, N.N.S.N.M. Kamal, Cytotoxicity and genotoxicity of biogenic silver nanoparticles in A549 and BEAS-2B cell lines, Bioinorg. Chem. Appl. (2022) 8546079, https://doi.org/10.1155/2022/8546079.

[8] S. Meenakshisundaram, V. Krishnamoorthy, Y. Jagadeesan, R. Vilwanathan, A. Balaiah, Annona muricata assisted biogenic synthesis of silver nanoparticles regulates cell cycle arrest in NSCLC cell lines, Bioorg. Chem. 95 (2020) 103451, https://doi.org/10.1016/j.bioorg.2019.103451.

[9] Baker Abu, S. Iram, A. Syed, A.M. Elgorban, A.H. Bahkali, K. Ahmad, M.S. Khan, J. Kim, Fruit derived potentially bioactive bioengineered silver nanoparticles, Int. J. Nanomedicine. 16 (2021) 7711–7726, https://doi.org/10.2147/IJN.S330763.

[10] H. Singh, J. Du, P. Singh, T.H. Yi, Ecofriendly synthesis of silver and gold nanoparticles by Euphrasia officinalis leaf extract and its biomedical applications, Artif. Cells, Nanomedicine, Biotechnol. 46 (2018) 1163–1170, https://doi.org/10.1080/21691401.2017.1362417.

[11] V.S. Shaniba, A.A. Aziz, P.R. Jayasree, P.R.M. Kumar, Manilkara zapota (L.) P. Royen leaf extract derived silver nanoparticles induce apoptosis in human colorectal carcinoma cells without affecting human lymphocytes or erythrocytes, Biol. Trace Elem. Res. 192 (2019) 160–174, https://doi.org/10.1007/s12011-019-1653-6.

[12] X. Hu, K. Saravanakumar, T. Jin, M.-H. Wang, Mycosynthesis, characterization, anticancer and antibacterial activity of silver nanoparticles from endophytic fungus Talaromyces purpureogenus, Int. J. Nanomedicine. 14 (2019) 3427–3438, https://doi.org/10.2147/IJN.S200817.

[13] N.N. Fard, H. Noorbazargan, A. Mirzaie, M.H. Ch, Z. Moghimiyan, A. Rahimi, Biogenic synthesis of AgNPs using Artemisia oliveriana extract and their biological activities for an effective treatment of lung cancer, Artif, Cells Nanomedicine Biotechnol. 46 (2018) S1047–S1058, https://doi.org/10.1080/21691401.2018.1528983.

[14] A. Zaki, M.N. Aziz, R. Ahmad, I. Ahamad, M.S. Ali, D. Yasin, B. Afzal, S.M. Ali, A. Chopra, V. Hadda, P. Srivastava, R. Kumar, T. Fatma, Synthesis, purification and characterization of Plectonema derived AgNPs with elucidation of the role of protein in nanoparticle stabilization, RSC Adv. 12 (2022) 2497–2510, https://doi.org/10.1039/d1ra08396a.

[15] S. Ahmed Annu, G. Kaur, P. Sharma, S. Singh, S. Ikram, Evaluation of the antioxidant, antibacterial and anticancer (lung cancer cell line A549) activity of Punica granatum mediated silver nanoparticles, Toxicol. Res. 7 (2018) 923–930, https://doi.org/10.1039/c8tx00103k.

[16] Q.H. Xia, Y.J. Ma, J.W. Wang, Biosynthesis of silver nanoparticles using Taxus yunnanensis callus and their antibacterial activity and cytotoxicity in human cancer cells, Nanomater 6 (2016) 160, https://doi.org/10.3390/nano6090160.

[17] V.N. Ivanov, A. Bhoumik, M. Krasilnikov, D. Levy, C.M. Horvath, Z. Ronai, Cooperation between STAT3 and c-jun suppresses fas transcription, Mol. Cell. 7 (2001) 517–528, https://doi.org/10.1016/S1097-2765(01)00199-X.

[18] J. V Alvarez, H. Greulich, W.R. Sellers, M. Meyerson, D.A. Frank, Signal Transducer and Activator of Transcription 3 Is Required for the Oncogenic Effects of Non – Small-Cell Lung Cancer – Associated Mutations of the Epidermal Growth Factor Receptor, 2006, pp. 3162–3168, https://doi.org/10.1158/0008-5472.CAN-05-3757.

[19] P. Dutta, N. Sabri, J. Li, W.X. Li, Role of STAT3 in lung cancer, JAK-STAT 3 (2014) e999503, https://doi.org/10.1080/21623996.2014.999503.

[20] J. Zhang, Y. Song, Y. Liang, H. Zou, P. Zuo, M. Yan, S. Jing, T. Li, Y. Wang, D. Li, T. Zhang, Z. Wei, Cucurbitacin IIa interferes with EGFR-MAPK signaling pathway leads to proliferation inhibition in A549 cells, Food Chem. Toxicol. 132 (2019) 110654, https://doi.org/10.1016/j.fct.2019.110654.

[21] A. Fehaid, R. Fujii, T. Sato, A. Taniguchi, Silver nanoparticles affect the inflammatory response in a lung epithelial cell line, Open Biotechnol. J. 14 (2020) 113–123, https://doi.org/10.2174/1874070702014010113.

[22] E.-J. Park, E. Bae, J. Yi, Y. Kim, K. Choi, S.H. Lee, J. Yoon, B.C. Lee, K. Park, Repeated-dose toxicity and inflammatory responses in mice by oral administration of silver nanoparticles, Environ. Toxicol. Pharmacol. 30 (2010) 162–168, https://doi.org/10.1016/j.etap.2010.05.004.

[23] M. Cascione, L. Rizzello, D. Manno, A. Serra, V. De Matteis, Green silver nanoparticles promote inflammation shutdown in human leukemic monocytes, Materials 15 (2022) 775, https://doi.org/10.3390/ma15030775.

[24] A.A.H. Abdellatif, S.K. Osman, M. Alsharidah, O. Al Rugaie, T.M. Faris, A. Alqasoumi, A.M. Mousa, A. Bouazzaoui, Green synthesis of silver nanoparticles reduced with Trigonella foenum-graecum and their effect on tumor necrosis factor-α in MCF7 cells, Eur. Rev. Med. Pharmacol. Sci. 26 (2022) 5529–5539.

[25] I. Chowdhury, B. Tharakan, G.K. Bhat, Caspases - an update, Comp. Biochem. Physiol., Part B: Biochem. Mol. Biol. 151 (2008) 10–27, https://doi.org/10.1016/j.cbpb.2008.05.010.

[26] M.L. Schrijvers, W.J. Pattje, M. Sc, L. Slagter-menkema, B. Sc, M.F. Mastik, B. Sc, J. H. Gibcus, D. Ph, J.A. Langendijk, D. Ph, J.E. Van Der Wal, D. Ph, B.F.A.M. Van Der Laan, D. Ph, E. Schuuring, D. Ph, Clinical investigation : head and neck cancer FADD expression as a prognosticator in early-stage glottic squamous cell carcinoma of the larynx treated primarily with radiotherapy, Radiat. Oncol. Biol. 83 (2012) 1220–1226, https://doi.org/10.1016/j.ijrobp.2011.09.060.